Microbial iron transport via a siderophore shuttle: A membrane ion transport paradigm

Alain Stintzi, Carmen Barnes, Jide Xu, and Kenneth N. Raymond*

Department of Chemistry, University of California, Berkeley, CA 94720-1460

Contributed by Kenneth N. Raymond, July 10, 2000

A mechanism of ion transport across membranes is reported. Microbial transport of Fe^{3+} generally delivers iron, a growth-limiting nutrient, to cells via highly specific siderophore-mediated transport systems. In contrast, iron transport in the fresh water bacterium *Aeromonas hydrophila* is found to occur by means of an indiscriminant siderophore transport system composed of a single multifunctional receptor. It is shown that (*i*) the siderophore and Fe^{3+} enter the bacterium together, (*ii*) a ligand exchange step occurs in the course of the transport, and (*iii*) a redox process is not involved in iron exchange. To the best of our knowledge, there have been no other reports of a ligand exchange mechanism in bacterial iron transport. The ligand exchange step occurs at the cell surface and involves the exchange of iron from a ferric siderophore to an iron-free siderophore already bound to the receptor. This ligand exchange mechanism is also found in *Escherichia coli* and seems likely to be widely distributed among microorganisms.

The significance of iron availability to microbial growth is evinced by two dramatic examples from widely different areas of environmental and medical biology. (*i*) Marine phytoplankton, which lie at the base of the biomass of the oceans, usually have iron as their growth-limiting nutrient. In two large-scale experiments in the open ocean, the addition of soluble, chelated iron caused an increase in biomass of 20 orders of magnitude (1, 2). (*ii*) Bacterial pathogens require iron and use siderophores, low-molecular-weight chelators, to solubilize and acquire iron. An inoculum of *Yersinia enterocolitica* with a 50% chance of producing a lethal microbial culture in mice, administered by peritoneal injection, is reduced from 10^8 to only 10 cells when the injection includes the iron complex of the siderophore desferrioxamine (3). The reason for these dramatic effects is that, whereas iron is the fourth most abundant element on earth, its bioavailability is extremely limited because of its poor solubility. At physiological pH, free $[Fe^{3+}]$ is limited to 10^{-18} M, whereas virtually all living microorganisms require a minimum effective concentration of 10^{-8} M for growth (4). Typically, this nutritional limitation is overcome by synthesizing and excreting siderophores, which occur in four broad groups based on the chemical nature of the chelating ligands: catecholates, hydroxamates, hydroxypyridonates, or aminocarboxylates (4–7).

In the last 10 years, much has been learned about the mechanism of iron acquisition and transport in Gram-negative bacteria, especially *Escherichia coli* (8–11). In these bacteria, the ferric-siderophore complex must cross the outer membrane and the cytoplasmic membrane before delivering iron within the cytoplasm. The ferric complexes are too large for passive diffusion or nonspecific transport across these membranes (4); ferric-siderophore uptake is both receptor and energy dependent. Translocation of iron through the bacterial outer membrane as the ferric-siderophore requires the formation of an energy-transducing complex with the proteins TonB, ExbB, and ExbD, which couple the electrochemical gradient across the cytoplasmic membrane to a highly specific receptor and so promote transport of the iron complex across the outer membrane (4, 9, 12, 13). Once in the periplasmic space, the ferric-siderophore binds to its cognate periplasmic binding protein and is then actively transported across the cytoplasmic membrane by an ATP-transporter system. The ferric-enterobactin and ferrichrome outer membrane receptors from *E. coli* (FepA and FhuA, respectively) have been extensively studied (10, 11). And the crystal structures of both receptors have been solved recently (14–16). These structures reveal two distinct functional domains: a 22-stranded antiparallel β-barrel, and an N-terminal globular domain, which folds inside the β-barrel, plugging the barrel pore. This structure is believed to be a common feature of any ferric-siderophore receptor and has been proposed to function like an air lock, involving two hatches (Fig. 1). The first hatch consists of the extracellular loops, which connect the strands of the barrel and fold toward the center of the pore, whereas the second hatch is formed by the N-terminal globular domain. Binding of the ferric-siderophore to its recognition site leads to closure of the external loops (first hatch) and opening of a channel in the periplasmic side of the membrane (second hatch), allowing the transit of the ferric-siderophore complex. These structural modifications are believed to be both ferric-siderophore and TonB induced (10). Indeed, a conformational change of the secondary structure of the N-terminal sequence of the protein, which switches from a helix to an unwound structure, has been observed upon binding of ferric-siderophore to FhuA and has been proposed to signal the receptor-loading status to the protein TonB (15, 16). Whether TonB induces a second conformational change (such as opening of a channel in the N-terminal globular domain) is not known, but the strict requirement of TonB in ferric-siderophore transport is undeniable. Despite this recent structural elucidation of these two receptors, the molecular basis of the mechanism of ferric-siderophore transport remains hypothetical and obscure.

The binding and transport of a ferric-siderophore to its receptor is usually highly specific, with a dissociation constant, K_d, in the range of 0.1 to 100 nM (11, 13). As an example, ferric-enterobactin binds avidly to its cognate receptor, FepA, with a K_d lower than 0.1 nM (17). Nevertheless, there is no doubt that certain receptors present lower affinity than others. For example, FhuE transports iron in *E. coli* via the hydroxamate siderophores coprogen, rhodotorulic acid, or ferrioxamine B (18). (Note that, whereas this receptor recognizes different siderophores, their structures are closely related and very similar at the iron coordination site.) Siderophore analogs have been used extensively to probe the role of the siderophore structure with regard to recognition by its receptor. The intensive study of ferric-enterobactin and FepA recognition (19–21) showed that the catechoylamide region of the ferric-enterobactin complex is recognized by the receptor FepA.

Here, we examine, with a similar approach, the specificity of the ferric-siderophore uptake system in a fresh water bacterium,

Abbreviation: DFO, deferriferrioxamine B.

*To whom reprint requests should be addressed. E-mail: Raymond@socrates.berkeley.edu.

The publication costs of this article were defrayed in part by page charge payment. This article must therefore be hereby marked "*advertisement*" in accordance with 18 U.S.C. §1734 solely to indicate this fact.

Article published online before print: *Proc. Natl. Acad. Sci. USA*, 10.1073/pnas.200318797. Article and publication date are at www.pnas.org/cgi/doi/10.1073/pnas.200318797

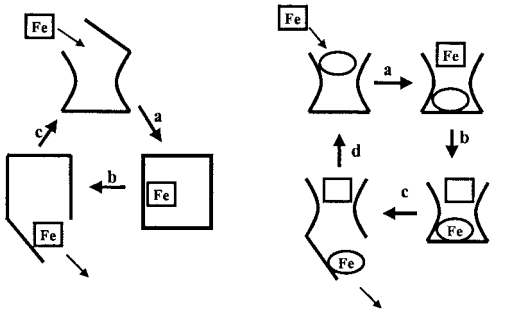

Fig. 1. (*Left*) The usual siderophore iron delivery mechanism: a, ferric siderophore is bound to the protein receptor, causing a conformational change in the protein; b, the ferric siderophore is pumped through the receptor into the periplasmic space; and c, on release of the ferric siderophore, the receptor protein returns to its original conformation. (*Right*) The siderophore shuttle iron delivery mechanism: a, with the iron-free siderophore initially bound to the receptor protein, a second, iron-loaded siderophore binds to the receptor; b, iron exchange between the two siderophores occurs; c, this iron exchange causes a conformational change and the iron complex of the originally iron-free siderophore enters the cytoplasm; d, on release of the ferric siderophore, the receptor protein returns to its original conformation, now with the originally iron-loaded siderophore bound to the receptor protein.

Aeromonas hydrophila. However, we find that *A. hydrophila* possesses a single receptor that is able to recognize and transport an extraordinarily broad range of siderophores, with chelating groups as varied as catecholate, hydroxamate or hydroxypyridonate (Fig. 2). Furthermore, this receptor utilizes an iron exchange uptake mechanism, involving exchange of iron from ferric-siderophore to an iron-free siderophore bound to the receptor (the shuttle mechanism of Fig. 1). This is a new kind of ion membrane transport mechanism and, as an iron acquisition strategy, seems likely to be quite widespread in Gram-negative bacteria.

Materials and Methods

Strains and Growth Conditions. The strain of *A. hydrophila* 495A2 and the amonabactin-deficient strain SB22 were from the laboratory of Dr. R. Byers and were grown in an iron-depleted synthetic medium (glucose mineral-salt medium), at 37°C under agitation 250 rpm. The glucose mineral-salt medium is composed of (per liter): 5.0 g glucose, 1.0 g $(NH_4)_2HPO_4$, 4.0 g K_2HPO_4, and 2.7 g KH_2PO_4. This growth medium was first made iron depleted by passing through a chelex100 (Bio-Rad) column, then supplemented with aqueous solutions of $MgSO_4$ and $MnSO_4$ to obtain a final concentration of 830 mM and 40 mM respectively, and finally filter sterilized (Millipore filters unit, pore diameter 0.22 mm).

The three strains of *E. coli* K-12, RW1318 (*fepA entA thi proC leu trp*), H1594 (*fiu:Mu* d1X *aroB aroD139 lacU169 rpsL thiA*), and HN593 (*cir fiu:Mu* d1X *aroB aroD139 lacU169 rpsL thiA*) (22), were obtained from Dr. H. Nikaido, University of California at Berkeley). *E. coli* strains were grown in glucose mineral-salt medium supplemented with the adequate amino acids and vitamins.

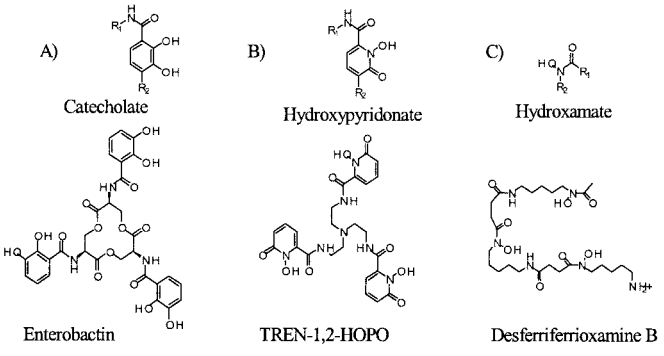

Fig. 2. Structures of iron chelating functionalities and representative siderophores. (*A*) Catecholate group and the enterobactin, siderophore produced by *E. coli*; (*B*) hydroxypyridonate group and the TREN-1,2-HOPO, synthetic siderophore analog; (*C*) hydroxamate group and the desferriferrioxamine B (DFO), siderophore produced by *S. pylosus*.

Siderophore Purification. Amonabactin was isolated from a culture of *A. hydrophila* 495A2 as previously described (23). Enterobactin was purified from the growth supernatant of *E. coli* AN311 after a published protocol (24). Cepabactin and corynebactin were gifts from Dr. Jean-Marie Meyer (Université Louis-Pasteur, Strasbourg, France). Rhodotorulic acid, alcaligin, coprogen, and ferrichrome were isolated from bacterial growth supernatant according to published procedures (25–28). Maltol was purchased from Aldrich. Syntheses of siderophore analogs, TRENCAM (29), TREN-1,2-HOPO (J.X. and K.N.R., unpublished data), deferiprone (30), and allo-maltol (31) have been described previously. Both maltol and allo-maltol were used in iron uptake experiments.

Synthesis of ^{55}Fe Complexes of Siderophores. Siderophore iron complexes were synthesized by mixing a solution of $^{55}FeCl_3$ (NEN) and siderophore with a ratio 1:1, 2:3, or 1:3 for, respectively, a hexadentate, tetradentate or bidentate siderophore. This solution was incubated at room temperature for 2 h, and free iron was removed by precipitation after the addition of a solution of sodium phosphate 0.5 M and centrifugation at 14,000 rpm for 10 min. Radioactive ^{55}Fe-siderophore complexes were filtered twice through membrane filters (HAWP Millipore, 0.45-mm pore size), and their concentrations were determined by monitoring the radioactivity by using a Packard scintillation counter.

Synthesis of Chromium Complexes of Siderophores. The Cr^{3+} complex of deferriferrioxamine B (DFO) was synthesized as described previously (32). The Cr^{3+}-TREN-1,2-HOPO complex was synthesized as follows: $CrCl_3 \cdot 6H_2O$ (22 mg,140 mmol) TREN-1,2-HOPO·HCl (105 mg, 167 mmol), and 2 equivalents of KOH (3.22 ml of a standardized 0.1037 M in methanol) were dissolved in water (20 ml). The remaining two equivalents of KOH (3.22 ml, 0.1037 M in methanol) were added dropwise with stirring, continuing for an hour at room temperature. The precipitated product was filtered or extracted into chloroform and dried *in vacuo*. The solid was resuspended into methylene chloride and further purified on a silica column (95:5 CH_2Cl_2, MeOH). A single spot was observed on silica TLC ($R_f = 0.35$ in 95:5 CH_2Cl_2, MeOH). The chromic and iron complexes had identical R_f values. FABMS+ m/z 607.2 (607.1 calculated for MH^+). The ^{51}Cr complex of desferriferrioxamine B was prepared by using Cr(II) from Zn/Hg amalgam as follows: methanol was distilled over calcium hydride, and the reaction was performed under nitrogen. Zinc metal pellets were extensively washed with dilute acid (0.1 M HCl) followed by water, then coated (mercuric nitrate in dilute nitric acid). The coated pellets were placed on a column (5 cm^3) and thoroughly rinsed, first with water and subsequently with dry methanol. An acidic solution of $^{51}CrCl_3$ (in 0.5 M HCl) and cold $CrCl_3 \cdot 6H_2O$ (10 mg, 63 mmol, 11.2 mCi/mmol) in methanol was added to the ZnHg column and kept there until the reduction of Cr(III) to Cr(II) was complete (the solution changed color from emerald green to light blue). The chromium solution was then added to a methanolic solution of desferriferrioxamine B (50 mg, 75.6 mmol) and

anhydrous sodium acetate (75 mg, 910 mmol). The reaction was then opened to air, allowing the chromium DFO complex to reoxidize (the solution changed from red to sea green) and was then concentrated to dryness by using a stream of N_2. The solid was resuspended in distilled water, applied to an XAD-2 resin (200–250 mesh), and washed thoroughly with water. The ^{51}CrDFO complex was eluted with 50% MeOH/H_2O, the methanol was evaporated, and the water was removed by lyophilization. The cold chromium complex of DFO was prepared the same way: FABMS+ m/z 610.5 (610.7 calculated for MH^+). The radiolabeled ^{51}Cr (TREN-1,2-HOPO) was prepared as described for the cold Cr (TREN-1,2-HOPO); $^{51}CrCl_3$ (in 0.5 M HCl) and cold $CrCl_3$ hexahydrate were mixed to a final concentration of (64.5 mCi/mmol).

Synthesis of ^{14}C-LysineCAM Siderophore Analog. The ^{14}C labeled L-lysineCAM was prepared as follows: to a solution of ^{14}C-L-lysine monohydrochloride (ICN, 0.05 mCi, 1.55×10^{-4} mmol) in 2% ethanol (0.5 ml), nonradioactive L-lysine (5 mg, 0.12 mmol) and ethanol (0.5 ml) were added. To the above lysine solution was added a solution of 2,3-dibenzyloxy-1-(2-mercaptothiazolide)benzamide (50 mg, 11.5 mmol) in methylene chloride (1 ml) followed by triethylamine (0.3 ml). This mixture was stirred at room temperature for 3 days. The solvent was removed under vacuo, and the residue was dissolved in methylene chloride (2 ml), extracted twice with 1 M HCl solution (1 ml), and purified by a mini flash silica gel column (1 g silica gel). The benzyl-protected ^{14}C-labeled L-lysineCAM was obtained as a pale yellow oil, yielding 16.6 mg (78%), which was characterized by ^{1}H and ^{13}C NMR (500 MHz, $CDCl_3$, 25°C). It was then deprotected by stirring with 1:1 mixture of concentrated HCl and glacial acetic acid for 3 days, the volatiles were removed under vacuo, and the residue was recrystallized from methanol/ether to give the ^{14}C-labeled L-lysineCAM as a beige solid, yielding 8.2 mg (92%). The total radioactivity of the product was found to be higher than 0.035 mCi, and the chemical structure of the product was confirmed by ^{1}H and ^{13}C NMR (500 MHz, DMSO-d_6, 25°C).

Siderophore Binding and Transport Experiments. *A. hydrophila* was grown in an iron starvation medium as previously described (23). After 18 h, the bacteria were harvested, washed, and resuspended in the medium to an optical density at 600 nm of 0.3. Bacterial suspension (9 ml) was incubated 5 min at 37°C, and transport assays were started by addition of ^{55}Fe-siderophore (1 ml). Aliquots of 1 ml were removed at set intervals, filtered through membrane filters (HAWP Millipore, 0.45-mm pore size), and washed with 10 ml of a cold solution of 0.1 M citrate. The filters were dried, collected in vials, and suspended in 6 ml of liquid scintillation UltimaGold XR (Packard). The vials were vigorously shaken and stored for 12 h, and the radioactivity was determined by using a Packard scintillation counter. For binding studies, bacterial suspensions, previously incubated on ice for 2 h, were supplemented with different concentrations of ferric-siderophore complexes or iron-free ^{14}C-lysineCAM siderophore analog. After 10 min, cells were filtered, washed, and counted as described. The binding and uptake data were analyzed by using ORIGIN 6 software (34).

Results and Discussion

Amonabactin-Mediated Iron Transport in *A. hydrophila*. In response to iron starvation, *A. hydrophila* strain 495A2 produces four bis-catecholate siderophores, collectively named amonabactins (34) (Fig. 3). These are composed of an amino acid backbone containing two lysines, one phenylalanine or tryptophane, and an optional glycine. Two 2,3-dihydroxybenzoyl groups are attached via N^{ε} amide linkages to the C terminus of lysine and to the N terminus of glycine or lysine. These two catecholate groups constitute the iron-chelating functionalities of amonabactins.

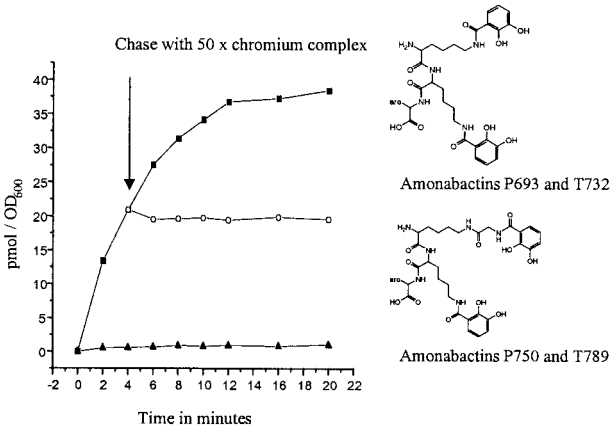

Fig. 3. Time-dependent uptake of ^{55}Fe-amonabactin T732 (0.4 mM) into cells of *A. hydrophila* and the chemical structure of amonabactin T732 and P693 (aro = indole or phenyl, respectively) and amonabactin T789 and P750 (aro = indole or phenyl, respectively). Experimental conditions were as described in *Materials and Methods*. (■) Uptake of ^{55}Fe-amonabactin T732; (▲) uptake of ^{55}Fe-amonabactin T732 in the presence of 1 mM KCN (cells were also treated 15 min with 1 mM KCN before the uptake experiment); (○) uptake of ^{55}Fe-amonabactin T732 with a 50-fold excess of the chromic complex of DFO or TREN-1,2-HOPO, added immediately after the 4-min sample was removed (arrow).

Their capacity to mediate Fe^{3+} transport in *A. hydrophila* 495A2 was studied by following the uptake rate of ^{55}Fe-amonabactin for 20 min; addition of 1 mM KCN, which disrupts the cytoplasmic proton motive force, stops iron uptake (Fig. 3). No uptake was observed at 0°C or by using glucose-depleted cells (data not shown). Therefore, like other characterized siderophore-mediated iron transport systems, Fe^{3+} uptake in *A. hydrophila* is energy dependent.

Specificity of the Ferric-Amonabactin Uptake System. The ability of 20 heterologous siderophores and siderophore analogs to mediate iron transport in *A. hydrophila* was studied by using the ^{55}Fe-siderophore uptake assay (as described in *Materials and Methods*). Among the siderophores or siderophore analogs tested were maltol and allo-maltol, bis-catecholates (amonabactins), tris-catecholates (enterobactin, corynebactin and TREN-CAM), mono-hydroxypyridonates (cepabactin and deferiprone), tris-hydroxypyridonate (TREN-1,2-HOPO), bis-hydroxa-mates (rhodotorulic acid and alcaligin), and tris-hydroxamates (desferriferrioxamine B, coprogen, and ferrichrome). These were all found to mediate ^{55}Fe transport in *A. hydrophila* 495A2. Binding and transport characteristics of the amonabactins and three representatives of the other transported siderophores [one catecholate (enterobactin), one hydroxypyridonate (TREN-1,2-HOPO), and one hydroxamate (desferrioxamine)] are presented in Table 1. Surprisingly, unlike other siderophore transport systems, such as ferric-enterobactin uptake in *E. coli*, the amonabactin receptor of *A. hydrophila* is relatively low affinity (with a dissociation constant, K_d, more than 10-fold higher compared with ferric-enterobactin binding to its receptor FepA in *E. coli*), but it still transports iron at rates comparable to other ferric-siderophore uptake systems (Table 1). Enterobactin and TREN-1,2-HOPO have K_d, K_{max}, and V_{max} values similar to those found for the amonabactins, whereas ferrioxamine B binding is less specific, with a K_d and K_{max} twice as large, suggesting a preference of iron-catecholate or catecholate-like structures as an iron source.

To investigate whether single or multiple transport systems are responsible for this iron uptake in *A. hydrophila*, chromium complexes of desferriferrioxamine B (DFO) and TREN-1,2-

Table 1. Binding and transport characteristics of ferric-amonabactin uptake system in *A. hydrophila* 495A2

Siderophore	Binding results K_d, nM	Transport results K_{max}, μM	Transport results V_{max}, pmol/min/OD_{600}
Amonabactin P683	800	3.6	24
Amonabactin P750	845	2.6	22
Amonabactin T732	832	3.0	19
Amonabactin T789	903	3.2	42
Enterobactin	820	4.0	24
Ferrioxamine B	1,604	11.4	7.1
TRENCAM	1,620	6.0	4.2
TREN-1,2-HOPO	804	4.0	20

Values of the two kinetic parameters, K_{max} (Michaelis constant) and V_{max} (maximum rate of transport) are calculated as the mean of three independent assays and are determined from plots of 1/*V* vs. 1/*S*, where *V* is the uptake rate and *S* the ferric-siderophore concentration. Binding experiments were carried out at 0°C by using an amonabactin-deficient strain of *A. hydrophila* 495A2. The K_d values were determined from the concentration dependence of ferric-siderophore binding as the mean of three independent experiments.

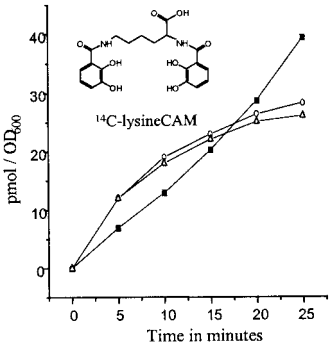

Fig. 4. Time-dependent uptake of ^{55}Fe-^{14}C-lysineCAM siderophore analog into cells of *A. hydrophila*. Conditions were as described in *Materials and Methods* except that the final complex concentration was 5 mM, cells were suspended in transport medium (30 ml) to an optical density of 1.2, and 5-ml aliquots were removed at each time and the radioactivity counted. The rate of ^{55}Fe (■) and ^{14}C (○) uptake were monitored simultaneously in the same assay by two-channel analysis. The rate of gallium-^{14}C-lysineCAM (△) uptake was monitored by following the transport of carbon 14.

HOPO were synthesized and used as probes for inhibition of ferric siderophore transport. These Cr^{3+} complexes are kinetically inert but similar in structure to those of Fe^{3+} complexes. The uptake of each ^{55}Fe-siderophore complex was monitored for 20 min. The Cr^{3+} complexes of DFO and TREN-1,2-HOPO were usually competitive inhibitors (as shown for amonabactin uptake, Fig. 3). Remarkably, the Cr^{3+} complexes inhibit the transport of the ferric complex of the four different amonabactins (Fig. 3), as well as cepabactin, enterobactin, corynebactin, ferrichrome, DFO, TRENCAM, TREN-1,2-HOPO, deferiprone, maltol and allo-maltol. Thus, it appears that all of these siderophores use the same transport system to mediate iron uptake. In contrast, Cr^{3+}-DFO and Cr^{3+}-TREN-1,2-HOPO did not inhibit the transport of the ferric complexes of coprogen, alcaligin, or rhodotorulic acid, which apparently use their own route of entry into the bacterium. We conclude that *A. hydrophila* possesses a single, multifunctional ferric-siderophore transport mechanism that is able to recognize and transport ferric siderophore complexes with different molecular structures and denticity, different iron-chelating functionalities (catecholate, hydroxypyridonate, and hydroxamate), different number of iron centers (one or two), and different charges.

Mechanism of Ferric-Siderophores Transport in *A. hydrophila*. We consider the following possibilities for this multifunctional recognition of siderophores: (*i*) there is a single receptor with different recognition sites or a single receptor that recognizes a common structural feature between all of the different siderophores; (*ii*) there are many receptors but a common periplasmic binding protein; (*iii*) the ferric-siderophore delivers the iron to a surface-bound iron carrier (likely through a reduction process), with the siderophore itself remaining outside the cell, as is observed in some fungi (35) and *Listeria monocytogenes* (36); or (*iv*) there are several transport systems, but the protein TonB is present in limiting amount and is therefore unable to promote siderophore uptake. Our results show that there is a single receptor, as we now describe.

The TonB protein is essential for the transport of ferric-siderophore complexes (12, 37, 38). Therefore, if an excess of chromium DFO or chromium TREN-1,2-HOPO complex induced binding of all of the available TonB proteins to their receptors, the transport of other ferric-siderophores would be inhibited, even if they were transported by using a different receptor. However the uptake of three ferric siderophore complexes (coprogen, alcaligin, and rhodotorulic acid) were not inhibited by the addition of an excess of chromium complex. This indicates that TonB is not present in limiting quantities, ruling out possibility *iv*.

To further establish whether the siderophore and Fe^{3+} enter the bacterium together, a bis-catecholate ^{14}C-siderophore analog, lysineCAM, was prepared. The Cr^{3+} complexes of DFO and TREN-1,2-HOPO inhibit the transport of Fe-lysineCAM (data not shown). Thus, lysineCAM uses the same transport system as amonabactin to mediate iron transport in *A. hydrophila*. The uptake rate of ^{55}Fe and ^{14}C from the ^{55}Fe-^{14}C-lysineCAM complex was monitored for 25 min. As shown in Fig. 4, ^{14}C-siderophore is transported into the cell at the same rate as ^{55}Fe during the first 10 min in a 3:2 ratio of ^{14}C-siderophore/^{55}Fe. Hence, this bis-catecholate siderophore forms a 3:2 complex with ferric ion, and both siderophore and iron are initially taken up. However, after 10 min, the transport rate of ^{14}C-siderophore decreases, whereas that of ^{55}Fe remains unchanged, suggesting that ^{55}Fe is released from the siderophore inside the cell and the ^{14}C-siderophore is excreted back into the extracellular medium. The possible role of a redox process in this ferric-siderophore transport was tested by using Ga-^{14}C-lysineCAM (gallium has no stable divalent state and therefore cannot be reduced). The gallium complex was taken up by *A. hydrophila* at the same rate as the ferric complex (Fig. 4), implying that no reduction of the metal center is involved in this transport. The gallium uptake and the double labeling experiment with the ^{55}Fe complex rule out possibility *iii*.

The ferric metal center is the common structural feature among all of the different siderophores which are taken up by *A. hydrophila.* Therefore, recognition by a single receptor may imply sensing of the metal center, which can occur only through at least partial exchange between the bacterial receptor and the ferric-siderophore complex. The ^{51}Cr complexes of DFO and TREN-1,2-HOPO, which have K_d values identical to the corresponding ferric complexes (data not shown), were found not to be transported into the cells, indicating that these complexes block the outer membrane receptor on the cell surface, which rules out possibility *ii*. Thus, we report a ligand exchange step in siderophore-mediated microbial iron transport.

Siderophore-Mediated Iron Transport in *E. coli* Through a Ligand Exchange Mechanism. Is such a ligand exchange transport mechanism unique to *A. hydrophila*? To answer this question, we investigated the function of ligand exchange in siderophore-

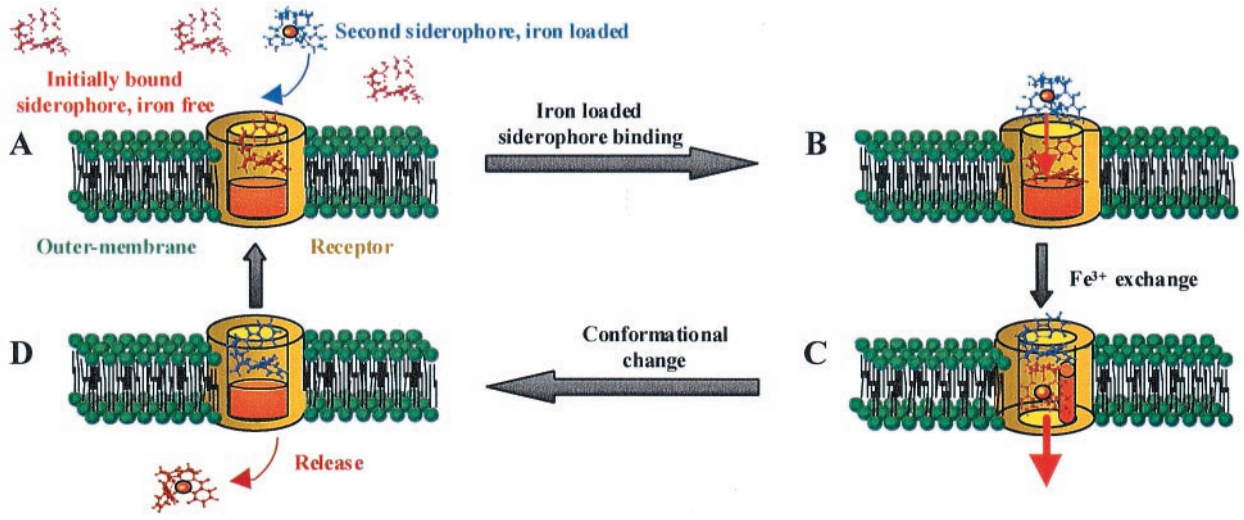

Fig. 5. Proposed model of the siderophore shuttle iron exchange mechanism for iron transport in Gram-negative bacteria. See text for a description of the steps involved in binding to the receptor, ligand exchange, and iron translocation.

mediated iron acquisition in *E. coli*. The double mutant *fiu cir* strains did not transport ^{55}Fe-TREN-1,2-HOPO, whereas both the *fepA*- and *fiu*-deficient strain did (data not shown). The ferric complex of TREN-1,2-HOPO mediates iron transport through the receptor Cir. The corresponding ^{51}Cr complex of TREN-1,2-HOPO inhibits the transport of its counterpart ferric complex and was found not to be transported in *E. coli* K-12 strain, clearly demonstrating that a ligand exchange mechanism is also responsible for iron acquisition in *E. coli*, via the protein Cir. However, microbes usually have more than one uptake mechanism. For example, *Ustilago sphaerogena*, *Streptomyces pilosus* and *Salmonella typhimurium* take up both the ligand and metal ion of Cr^{3+}-deferriferrichrome, Cr^{3+}-desferriferrioxamine B, and Cr^{3+}-deferriferrichrome, respectively. From our study, it appears that at least two different mechanisms for ferric-siderophore transport exist in these organisms: one involving ligand exchange and one which does not (Fig. 1).

Molecular Basis of the Ligand Exchange Mechanism. Because ligand exchange is a necessary step for this new iron transport system in *A. hydrophila* and the receptor must sense the metal center, two mechanistic possibilities can be proposed: (*i*) the receptor protein contains its own iron-chelating functionality (e.g., catechol or hydroxamate groups) because of a posttranslational modification, or (*ii*) an iron-chelating molecule, such as a free siderophore, avidly binds to the receptor protein, accelerating ferric ion exchange between the ferric-siderophore and the free siderophore bound to the receptor and completing iron transport.

Significantly, the iron-free ^{14}C-lysineCAM siderophore analog was found to have the same affinity for the receptor as its ferric complex, with a K_d (obtained by using whole cells of *A. hydrophila*) of 660 and 792 nM and a maximum capacity binding of 156 and 158 pmol/OD_{600} for the free and complexed siderophore, respectively. In addition, Schalk and collaborators reported the copurification of the ferric-siderophore receptor of *Pseudomonas aeruginosa* with its iron-free ligand (39). These findings suggested to us a mechanism of iron transport via a receptor loaded with its iron-free siderophore. Thus, we investigated whether Fe^{3+} in iron-loaded siderophore can be exchanged with the iron-free siderophore bound to the receptor *in vivo*. Bacterial cells (OD_{600} = 6) were incubated on ice with iron-free ^{14}C-lysineCAM siderophore analogs (3.10^{-8} mol) for 5 min, corresponding to the first binding step. Unbound ^{14}C-lysineCAM siderophores were removed by centrifugation, and the cells were washed, resuspended in uptake medium with iron-loaded siderophore (ferric amonabactin, 1.5×10^{-7} mol), and incubated at 37°C to initiate the transport (experiment A). A similar experiment, but with the omission of iron-loaded siderophores, was carried out simultaneously (experiment B). After 2 min, bacteria were harvested by centrifugation and resuspended in cold growth medium to perform a second binding step by adding iron-free ^{14}C-lysineCAM siderophore analog (3.10^{-8} mol). Finally the ^{14}C radioactivity, incorporated and bound to the cells, was monitored. The count obtained in experiment B, 5.2×10^{-10} per OD_{600} of ^{14}C-lysineCAM, corresponds to the quantity of ^{14}C-lysineCAM siderophores that bind to the cells. In experiment A, either the iron-loaded siderophore exchanges its iron with the iron-free ^{14}C-lysineCAM siderophore bound to the receptor, allowing the transport of ^{14}C-lysineCAM into the cells, or the iron-loaded siderophore competes for the binding site with the iron-free ^{14}C-lysineCAM siderophore, resulting in the transport of the nonradioactive ferric siderophore. In experiment A, scintillation counting gave 10.5×10^{-10} mol of ^{14}C-lysineCAM siderophore per 1 OD_{600} of cells, which corresponds to exactly double the amount of the ^{14}C-lysineCAM siderophore able to bind to the cell surface. It is clear that the ^{14}C-lysineCAM siderophore bound to the membrane (as a result of the first binding step) has been transported into the cells, and this occurs only if the ^{14}C-lysineCAM has acquired iron because iron-free lysineCAM is not transported into *A. hydrophila* (data not shown). Thus, iron must exchange between the cold ferric-siderophore and the ^{14}C-lysineCAM bound to the receptor. Based on these results, and in light of the crystal structures of the two receptors, FepA and FhuA, we propose the following model of ferric-siderophore transport (Fig. 5). In Fig. 5*A in vivo*, iron-free siderophore (in red) is in large excess over iron-loaded siderophore (in blue) and consequently predominates as bound to its cognate receptor. The crystal structures of FepA (14) and FhuA (15, 16) receptors reveal two distinct functional domains, which are believed to be a common feature of any ferric-siderophore receptor: a 22-stranded anti-parallel β-barrel and an N-terminal globular domain that folds inside the β-barrel closing the barrel pore (Fig. 5*A*, represented in brown). Iron-loaded siderophore is brought close enough to the iron-free bound siderophore to promote the

exchange of iron (Fig. 5*B*, red arrow). This iron exchange is likely triggered by a pH gradient inside the barrel of the receptor, which results in the protonation of the donor and deprotonation of the acceptor. This process may be assisted by ternary complex formation involving receptor protein side chain donors. The ligand exchange induces a conformational change of the N-terminal globular domain (Fig. 5*B*, as represented in orange), signaling the iron-loaded status of the bound siderophore to the protein TonB (Fig. 5*C*). Energized TonB then triggers a conformational change of the receptor, allowing translocation of the ferric-siderophore from the cell surface to the periplasmic space. The ferric-siderophore that gave up its iron then binds to the receptor, replacing the transported ferric-siderophore complex (Fig. 5*D*). Finally, the receptor returns to its initial conformation. The net result is a shuttle mechanism in which siderophore ligands pass serially through a channel, with iron exchange between the siderophores a key step in the process (Fig. 1 *Right*). For the amonabactins, which form a 3:2 complex with ferric ion, it seems likely that the exchange of a single ligand will be enough to trigger the transport.

Conclusions

In summary, our study of amonabactin-mediated iron transport in *A. hydrophila* provides an example of a ligand exchange mechanism involved in bacterial iron acquisition. The ligand exchange step occurs at the cell surface and involves the exchange of iron from a ferric siderophore to an iron-free siderophore bound to the receptor. This mechanism suggests an increase of the iron uptake rate, with increasing concentration of iron-free siderophore (characteristic of ferric-siderophore poor environment of *in vivo* conditions). Indeed, preliminary experimental results support this role of iron-free siderophore as a catalyst for iron uptake at very low siderophore concentrations. Because most iron transport studies (including ours) have been done under higher iron loading conditions (significantly higher than aquatic organisms are likely to experience), this behavior has not been reported earlier. The ability to select for Fe^{3+} via ligand exchange enables production of a single receptor with a lower affinity for its cognate siderophore but with a broad range of siderophore recognition, as observed in *A. hydrophila*. In a medium with a low ferric-siderophore concentration, this iron acquisition strategy is more efficient than one in which iron is acquired via a set of receptors (usually inducible), each of which is specific to a single siderophore. Furthermore, a ligand exchange mechanism for iron acquisition provides the bacterium with the ability to steal iron from exogenous siderophores. This mechanism may give *A. hydrophila* a great advantage *in vivo*, because it avoids the costly loss of secreted siderophores and provides the bacterium with the ability rapidly to acquire iron whenever it is encountered (a particular problem for aquatic or marine habitats). Whereas this is a new mechanism for siderophore-mediated iron transport in bacteria, it also represents a generally new ion transport process. This mechanism, presently found in *A. hydrophila* and *E. coli*, explains the observations from Schalk and collaborators with *P. aeruginosa* (39) and probably those from Hutchins and collaborators (40), who recently observed the ability of the marine bacterium, *Synechococcus*, to acquire iron from catecholate, hydroxamate, or mixed functional group siderophores. We suggest that this siderophore shuttle transport mechanism may be widespread in bacteria.

Ref. 23 is the previous paper in this series, "Coordination Chemistry of Microbial Iron Transport Compounds." This research was supported by National Institutes of Health Grant AI 11744.

1. Frost, B. W. (1996) *Nature (London)* **383,** 475–476.
2. Coale, K. H., Johnson, K. S., Fitzwater, S. E., Gordon, R. M., Tanner, S., Chavez, F. P., Ferioli, L., Sakamoto, C., Rogers, P., Millero, F., *et al*. (1996) *Nature (London)* **383,** 495–501.
3. Robins-Browne, R. M. & Prpic, J. K. (1985) *Infect. Immun.* **47,** 774–779.
4. Braun, V. & Hantke, K. (1997) in *Transition Metals in Microbial Metabolism*, eds. Winkelmann, G. & Carrano, C. J. (Harwood, Amsterdam), pp. 81–101.
5. Neilands, J. B. (1995) *J. Biol. Chem.* **270,** 26723–26726.
6. Raymond, K. N., Müller, G. & Matzanke, B. F. (1984) in *Topics in Current Chemistry*, ed. Boschk, F. L. (Springer-Verlag, Berlin), pp. 50–97.
7. Telford, J. R. & Raymond, K. N. (1996) in *Comprehensive Supramolecular Chemistry*, eds. Atwood, J. L., Davies, J. E. D., MacNicol, D. D. & Vögtle, F. (Elsevier Science, Oxford), Vol. 1, pp. 245–266.
8. Braun, V. & Killmann, H. (1999) *Trends Biochem. Sci.* **24,** 104–109.
9. Braun, V. (1998) *Science* **282,** 2202–2203.
10. Braun, V., Kantke, K. & Koster, W. (1998) *Met. Ions Biol. Syst.* **35,** 67–145.
11. van der Helm, D. (1998) *Met. Ions Biol. Syst.* **35,** 355–401.
12. Moeck, G. S. & Coulton, J. W. (1998) *Mol. Microbiol.* **28,** 675–681.
13. Postle, K. (1999) *Nat. Struct. Biol.* **6,** 3–4.
14. Buchanan, S. K., Smith, B. S., Venkatramani, L., Xia, D., Esser, L., Palnitkar, M., Chakraborty, R., van der Helm, D. & Deisenhofer, J. (1999) *Nat. Struct. Biol.* **6,** 56–63.
15. Locher, K. P., Rees, B., Koebnik, R., Mitschler, A., Moulinier, L., Rosenbusch, J. P. & Moras, D. (1998) *Cell* **95,** 771–778.
16. Ferguson, A. D., Hofmann, E., Coulton, J. W., Dieterichs, K. & Welte, W. (1998) *Science* **282,** 2215–2220.
17. Newton, S. M. C., Igo, J. D., Scott, D. C. & Klebba, P. E. (1999) *Mol. Microbiol.* **32,** 1153–1165.
18. Hantke, K. (1983) *Mol. Gen. Genet.* **191,** 301–306.
19. Thulasiraman, P., Newton, S. M. C., Xu, J., Raymond, K. N., Mai, C., Hall, A., Montague, M. A. & Klebba, P. E. (1998) *J. Bacteriol.* **180,** 6689–6696.
20. Ecker, D. J., Loomis, L. D., Cass, M. E. & Raymond, K. N. (1988) *J. Am. Chem. Soc.* **110,** 2457–2464.
21. Ecker, D. J., Matzanke, B. F. & Raymond, K. N. (1986) *J. Bacteriol.* **167,** 666–673.
22. Nikaido, H. & Rosenberg, E. Y. (1990) *J. Bacteriol.* **172,** 1361–1367.
23. Stintzi, A. & Raymond, K. N. (2000) *J. Biol. Inorg. Chem.* **5,** 57–66.
24. Young, I. G. & Gibson, F. (1979) *Methods Enzymol.* **56,** 394–398.
25. Atkin, C. L. & Neilands, J. B. (1968) *Biochemistry* **7,** 3734–3739.
26. Moore, C. H., Foster, L. A., Gerbig, D. G. J., Dyer, D. W. & Gibson, B. W. (1995) *J. Bacteriol.* **177,** 1116–1118.
27. Wong, G. B., Kappel, M. J., Raymond, K. N., Matzanke, B. F. & Winkelmann, G. (1983) *J. Am. Chem. Soc.* **105,** 810–815.
28. Payne, S. M. (1994) *Methods Enzymol.* **235,** 329–344.
29. Rodgers, S. J., Lee, C.-W., Ng, C.-Y. & Raymond, K. N. (1997) *Inorg. Chem.* **26,** 1622–1625.
30. Harris, R. L. N. (1976) *Aust. J. Chem.* 1329–1334.
31. Thomas, A. F. & Marxer, A. (1960) *Helv. Chim. Acta* **43,** 469.
32. Müller, G. & Raymond, K. N. (1984) *J. Bacteriol.* **160,** 304–312.
33. Anonymous (1991–1999) ORIGIN 6 (Microcal Software, Northampton, MA).
34. Telford, J. R. & Raymond, K. N. (1997) *J. Biol. Inorg. Chem.* **2,** 750–761.
35. Howard, D. H. (1999) *Clin. Microbiol. Rev.* **12,** 394–404.
36. Coulanges, V., Andre, P., Ziegler, O., Buchheit, L. & Vidon, D. J. (1997) *Infect. Immun.* **65,** 2778–2785.
37. Klebba, P. E., Rutz, J. M., Liu, J. & Murphy, C. K. (1993) *J. Bioenerg. Biomembr.* **25,** 603–611.
38. Postle, K. (1993) *J. Bioenerg. Biomembr.* **25,** 591–601.
39. Schalk, I. J., Kyslik, P., Prome, D., van Dorsselaer, A., Poole, K., Abdallah, M. A. & Patus, F. (1999) *Biochemistry* **38,** 9357–9365.
40. Hutchins, D. A., Witter, A. E., Butler, A. & Luther, G. W. (1999) *Nature (London)* **400,** 858–861.